RSC Advances

PAPER

View Article Online
View Journal | View Issue

Cite this: *RSC Adv.*, 2022, **12**, 3763

Study on the mechanism of laccase-catalyzed polydopamine rapid dyeing and modification of silk†

Qingqing Zhou, *[ab] Wen Wu [a] and Tieling Xing [b]

Research on the polymerization of dopamine and its modification on the surface of materials has received extensive attention. In this work, the process of laccase catalyzing the rapid polymerization of dopamine and *in situ* dyeing of silk fabric were studied. The results showed that laccase catalyzed dyeing for 3 h under acidic conditions could achieve the dyeing effect of 24 h under an alkaline environment, and the enzyme catalyzed polydopamine showed better deposition uniformity on the substrate surface. According to molecular simulation analysis, dopamine oligomers were easily combined with the amorphous regions of silk fibroin, and dopamine oligomers and amino acids of silk fibroin could form hydrogen bonds and π–π stacking interactions. Dopamine oligomers could form intermolecular and intramolecular hydrogen bonds through amino groups and hydroxyl groups. In addition, dopamine oligomers would aggregate in the process of binding to silk fibroin and adsorbed to the surface of silk fibroin in the form of aggregates, and Michael addition reaction would also occur between dopamine oligomers and silk fibroin. Finally, the silk fabrics loaded with polydopamine were reacted with different kinds of metal salt solutions to form particles with different morphologies and crystal structures on the surface of the silk fibers, and the modified silk fabrics showed good hydrophobicity.

Received 3rd December 2021
Accepted 14th January 2022

DOI: 10.1039/d1ra08807f

rsc.li/rsc-advances

1. Introduction

Dopamine has reducibility, antibacterial properties and excellent adhesion. It could self-polymerize in an alkaline environment, and its polymerized products (polydopamine) could adhere to the surface of various substrates. The traditional polymerization process needed to react in an alkaline environment for 12 h or even one day.[1] However, many researchers had found that when strong oxidants and metal ions were added, dopamine could self-polymerize under acidic conditions.[2–4] In the traditional textile industry, protein fibers (such as silk and wool) were dyed under acidic conditions.[5,6] Strong oxidants would cause damage to the fibers, and metal ions would pollute the water. Therefore, the above reaction conditions of dopamine self-polymerization were not suitable for dyeing and functional finishing of protein fibers.

Laccase is a copper containing polyphenol oxidase produced by a variety of fungi, plants and bacteria. Its molecule contains four copper atoms, which can extract electrons from phenolic substrates, and reduce molecular oxygen to water.[7] Compared with other oxidases, laccase has been reported to be relatively nonspecific, and can catalyze the oxidation of a wide range of phenolic compounds and aromatic amines, while simultaneously reducing its oxygen-water co-substrate.[8] Its extensive substrate specificity makes it widely used in the fields of biofuel cells, biosensors, bioremediation and wastewater treatment.[9,10] In the textile field, laccase can be used for decolorization and detoxification of dye wastewater, finishing of jeans, bleaching of cotton fabric, scouring of roving and dyeing of protein fiber.[11–13] Wang Ping's group used laccase to catalyze the graft polymerization of aromatic amines such as aniline (ANI) and *p*-phenylenediamine (PPD) to dye and functionalize silk fabrics *in situ*.[14] The results showed that silk fabric could be endowed with high color depth, color fastness, antibacterial and antioxidant capacity. Fan *et al.* used laccase as catalyst to induce phenolic acid compounds to dye wool fabric.[15] By optimizing the monomer concentration and reaction time, a higher color depth was obtained, and the pre-treated wool fabrics had good levelness and color fastness. Phenolic compounds have good biological activity, medicinal property, antibacterial property, antioxidant property, and reducing activity.[16–20] Moreover, while the above laccase catalyzed polymerization of phenolic compounds and surface modification of the substrate, phenolic compounds were also successfully immobilized on the surface of the substrate, which can be used as a secondary reaction platform for subsequent modification of the substrate.[21] Since

[a]*Key Laboratory of Yarn Materials Forming and Composite Processing Technology of Zhejiang Province, Jiaxing University, Jiaxing 314001, China. E-mail: zhouqingqing716@163.com; Fax: +86-573-83640322; Tel: +86-573-83641175*

[b]*National Engineering Laboratory for Modern Silk, Soochow University, Suzhou 215123, China*

† Electronic supplementary information (ESI) available. See DOI: 10.1039/d1ra08807f

dopamine had the same catechol structure as natural phenolic compounds, laccase could catalyze the rapid oxidation and self-polymerization of dopamine to dye and finish the silk fabrics.

Therefore, this work studied the rapid polymerization of dopamine catalyzed by laccase under acidic conditions and compared the self-polymerization process under traditional alkaline conditions. At the same time, the effect of *in situ* dyeing modification of silk fabrics by dopamine under two polymerization conditions was also studied. In order to further study the process of dyeing silk fabrics with dopamine and its oligomers, a molecular model of silk fibroin and a variety of dopamine oligomer models were constructed. Molecular dynamics simulation was used to explore the form of dopamine oligomers bound to the surface of silk fibroin, and which parts of silk fibroin were more easily combined with dopamine oligomers. Subsequently, the modified silk fabrics were reacted with different metal salt solutions to construct rough structure on fiber surfaces, the crystal structure of particles on surfaces and the hydrophobicity of the silk fabrics were studied.

2. Experimental

2.1. Materials

Silk fabric (72 g m^{-2}) was provided by Jiangsu Huajia Group Co., Ltd., dopamine hydrochloride (AR) and tris(hydroxymethyl) aminomethane (AR) were purchased from SuZhou KeChuang Biotechnology Co., Ltd., laccase (from coriolus versicolor) and diammonium 2,2′-azino-bis(3-ethylbenzothiazoline-6-sulfonate) (ABTS, 98.0%) were obtained from Shanghai Yuanye Bio-Technology Co., Ltd., $CuSO_4 \cdot 5H_2O$ (AR), $AgNO_3$ (AR), $FeCl_3 \cdot 6H_2O$ (AR) and $Ni(CH_3COO)_2 \cdot 4H_2O$ (AR), acetic acid (AR) and sodium acetate (AR) were purchased from Sinopharm Chemical Reagent Co., Ltd. The fabric was washed with soap flakes at 60 °C and rinsed before use, and the other chemical reagents were used as they were received. The activity of laccase needed to be measured before the experiment, and the test method was consistent with the previous method used by our group.[22] In brief, ABTS was used to determine the activity of laccase by an oxidation method at 415 nm (ε = 29 300 M^{-1} cm^{-1}), and one laccase activity unit was defined as the amount of enzyme that transforms 1 μmol min^{-1} of ABTS at 25 °C.

2.2. Experimental methods

Laccase-catalyzed dopamine polymerization to modify silk fabric: laccase (0.5 U mL^{-1}) was added into the solution containing 2 g L^{-1} dopamine hydrochloride, and the pH value of the reaction system was adjusted to 3.5 with acetic acid buffer, the liquor ratio of silk fabric dyeing was 1 : 50 (g mL^{-1}), and the reaction was carried out in a constant temperature shaking dyeing machine at 50 °C for a certain time, then it was washed by deionized water for several times to remove the floating color and dried at 50 °C.

Modification of silk fabric by self-polymerization of dopamine under alkaline conditions: as in the previous literature,[23] the dopamine solution was conditioned to pH 8.5 with Tris buffer, and the silk fabric was placed into the above reaction system under the same liquor ratio as above for 24 h, the silk fabric needs to be turned from time to time during the dyeing process to ensure the dyeing effect more uniform (experience had learned that if the fabric was not turned constantly during this dyeing process, large staining plaques visible to the naked eye would be appeared on the surface of silk fabric), and then took it out to wash the floating color with deionized water, and dried at 50 °C.

The dyed silk fabrics were placed in different kinds of metal salt solutions with the concentration of 40 mmol L^{-1} respectively, after reaction at room temperature for 24 h, the fabrics were washed with deionized water and dried at 50 °C in vacuum.

2.3 Simulation and calculation method

The molecular models were constructed according to the typical structures of dopamine oligomers reported by Chai Dongliang *et al.*,[24] and the specific structures were shown in Fig. S1.† Because the experimental conditions in this article were acidic, the molecules containing primary amino groups were treated as amino cation. According to the method reported by Cheng Yuan *et al.*,[25] the protein structure was pre-equilibrated, and the protein structure after pre-equilibration was shown in Fig. 1.

The simulation system was set up according to the experimental process and parameters. One silk protein macromolecule, six dopamine dimers, nine dopamine tetramers, two dopamine octamers, 59 hydronium ions, 64 chloride ions and 172 539 water molecules were added to the system. One dopamine oligomer of each structure was added in the system, which could ensure the ergodicity for each type of the oligomers. The size of the system was set to 17.45 × 17.45 × 17.45 nm^3. The Amber99sb ildn force field parameters[26] were used for the silk protein. And GAFF force field parameters[27] were used for the dopamine oligomers. The RESP charges are used for the oligomers which were fitted by the Antechamber program with HF/6-31G*[28,29] method. The SPCE model was used for the water molecules. The parameters of hydronium ions and chloride ions were based on the work of Chew Alex K., *et al.*30 The steepest descent method was used to eliminate unreasonable contacts in the system, and then 400 ps of NVT and 1 ns of NPT pre-equilibrium simulation were carried out. Finally, 200 ns of constant temperature and pressure simulation was performed.

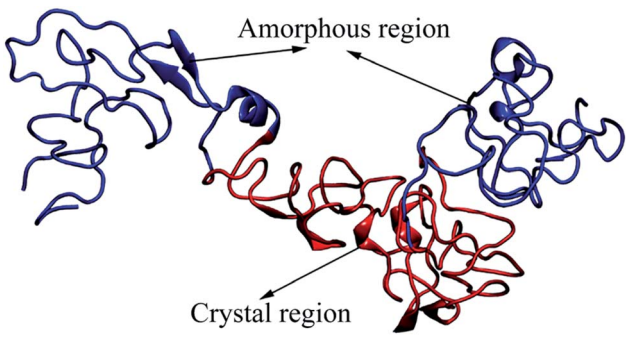

Fig. 1 The molecular structure of pre-equilibrated fibroin.

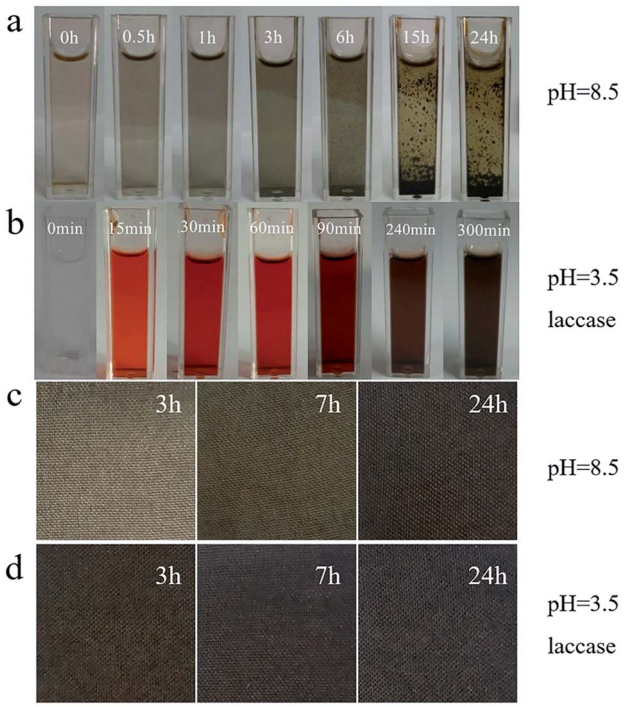

Fig. 2 (a) Self-polymerization of dopamine; (b) rapid polymerization of dopamine catalyzed by laccase; (c) modification of silk fabric by self-polymerization of dopamine; (d) modification of silk fabric by rapid polymerization of dopamine catalyzed by laccase.

The simulation integration method was frog leaping. The integration step was 2 fs. The neighbor list was updated every 10 steps and its cut-off value was 1.2 nm. The periodic boundary conditions were used in the three directions of *XYZ*. The cut-off value was 1.2 nm for van der Waals interactions. The PME method was used for electrostatic force. The simulated temperature was 50 °C, and the temperature coupling method was Nosé–Hoover; the simulated pressure was 1 atm, and the pressure coupling method was Parrinello–Rahman. To impose constraints on the bond length of all hydrogen atoms, the Lincs constraint method was used. The Gromacs 2018.2 program was used for the simulations and analyses, and the VMD 1.9.3 program was used for graphical display.

2.4 Characterizations

The K/S value of fabric was measured with a color matching instrument under D65 light source and 10° viewing angle, and the average value of five measurements was taken as the final K/S value. A field emission scanning electron microscope (FESEM, Hitachi S-4800) was used to observe the surface morphology of the silk fabrics under a voltage of 3.0 kV. The X-ray diffraction (XRD) patterns of the samples were tested using the Bruker D8 Advance diffractometer. The samples were tested with filtered CuKα radiation ($\lambda = 0.154$ nm) at a scanning speed of 2° min^{-1}, and the scanning range of the 2θ angle was 10° to 90°. The water contact angle of the silk fabric was evaluated using the German Krüss DSA 100 contact angle tester, the water droplet volume was 3 μL, and the test result was the average of 5 measurements. The X-ray photoelectron (XPS) spectra were measured by a Thermo Fisher Scientific Instrument (ESCALAB250Xi, USA) with an Al Kα X-ray source (1484.6 eV).

3. Results and discussion

3.1 Polymerization of dopamine and the dyeing modification of silk

Laccase was used to catalyze the polymerization of dopamine and to perform rapid dyeing modification of silk fabrics, and the modification effect was compared with traditional self-polymerization modification under alkaline conditions. It can be seen from Fig. 2a and b that it took 24 h for dopamine to self-polymerize in alkaline environment with pH 8.5 to get brownish black polymer, and the polymer was easy to aggregate and deposit to form large particles visible to naked eyes. While under the acidic conditions of pH = 3.5 and catalyzed by laccase, the polymerization rate was greatly increased, and the polymer solution was more uniform without obvious aggregates. Subsequently, the dyeing modification effects of silk were compared under the above polymerization conditions. As shown in Fig. 2c and d, dopamine can be rapidly polymerized under the catalysis of laccase and modify silk fabrics *in situ*, the K/S value of the fabric can reach 8.9 after 3 h. After being modified for 24 h under alkaline condition, the K/S value of silk fabric was 8.7, indicating that the efficiency of laccase catalyzing the rapid modification of silk fabrics with dopamine *in situ* was much higher than that of the traditional alkaline condition. And after comparing the results of 7 random multi-point measurements, the coefficient of variation of the K/S value of the silk fabric modified by the traditional method and the laccase-catalyzed method were 21.5% and 7.1%, respectively, indicating that the modification effect of laccase catalyzed polymerization was more homogeneous, which was also consistent with the effect of macro-visual observation of the polymer in the reaction solution above. Meanwhile, the silk fabric was acid-resistant but not alkali-resistant,[31,32] so laccase catalyzed dyeing modification under acidic conditions was more conducive to maintain the properties of silk fabrics.

Table 1 Color fastness of dyed silk fabrics

	Rubbing		Washing			
Property	Dry	Wet	Fading	Cotton staining	Silk staining	Light
Dyed silk fabric (laccase-catalyzed)	5	4–5	4	4–5	4–5	4
Dyed silk fabric (self-polymerization)	5	4	4	4–5	4	4

Table 2 Physical properties of the pristine silk fabric and the dyed silk fabric

Property	Pristine silk fabric	Dyed silk fabric (Laccase-catalyzed)	Dyed silk fabric (self-polymerization)
Tensile strength (N cm^{-1})	533.2 ± 34 (warp)	504.5 ± 32 (warp)	494.3 ± 33 (warp)
	392.7 ± 43 (weft)	413.2 ± 33 (weft)	387.1 ± 31 (weft)
Elongation at break (%)	42.3 ± 1.3 (warp)	40.3 ± 1.4 (warp)	39.2 ± 1.5 (warp)
	30.9 ± 0.8 (weft)	32.1 ± 0.5 (weft)	29.7 ± 0.9 (weft)

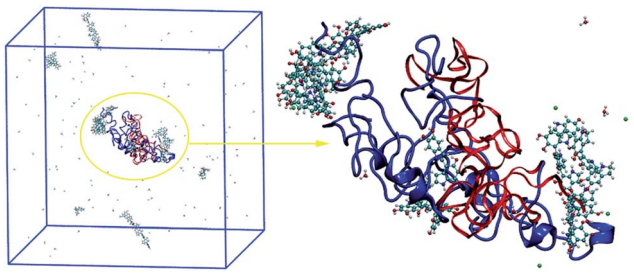

Fig. 3 The picture of the finial state of the system (water molecules are not shown).

In addition, the color fastness and mechanical properties of silk fabrics were also investigated. The color fastness test results were listed in Table 1. In general, the color fastness of silk fabrics dyed by the two methods was almost the same. They both had good rubbing fastness (grade 4–5) and color fastness to washing, but the light fastness was not good enough. As can be seen in Table 2, it was clear that the tensile strength and elongation at break of the enzymatic dyed silk fabrics decreased in the warp direction. However, in the weft direction, the tensile strength and elongation at break increased slightly, which may be attributed to the coating of polydopamine on the silk fibers. The abovementioned results showed that the laccase-catalyzed dyeing process had little effect on the overall mechanical properties of the silk fabrics. For the silk fabrics dyed by self-polymerization of dopamine in an alkaline condition, as silk was a kind of protein fiber, it was acid resistant but not alkali resistant. Long term exposure to alkaline environment would have an adverse effect on its macromolecules, so the mechanical properties of these silk fabrics were slightly reduced.

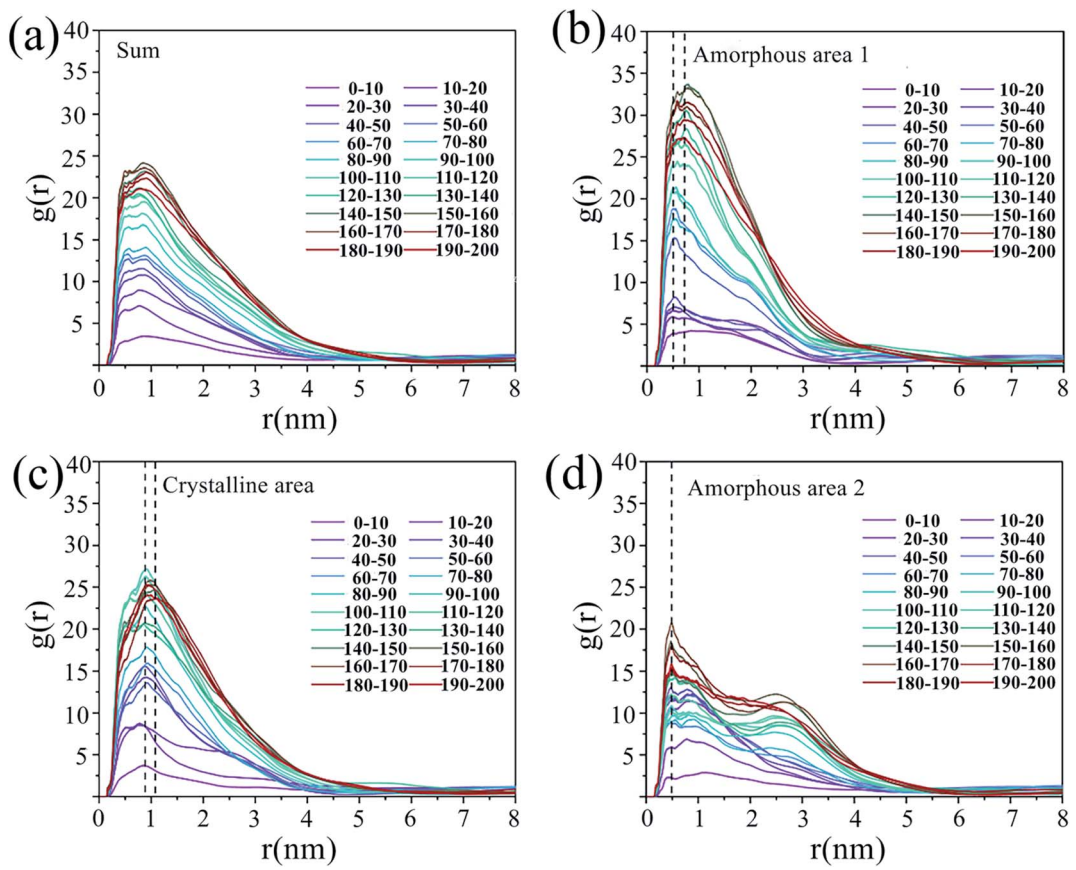

Fig. 4 The radial distribution functions of the dopamine oligomers around the silk fibroin in different time periods, the reference molecule: (a) the whole protein; (b) the amorphous area 1; (c) the crystalline area; (d) the amorphous area 2.

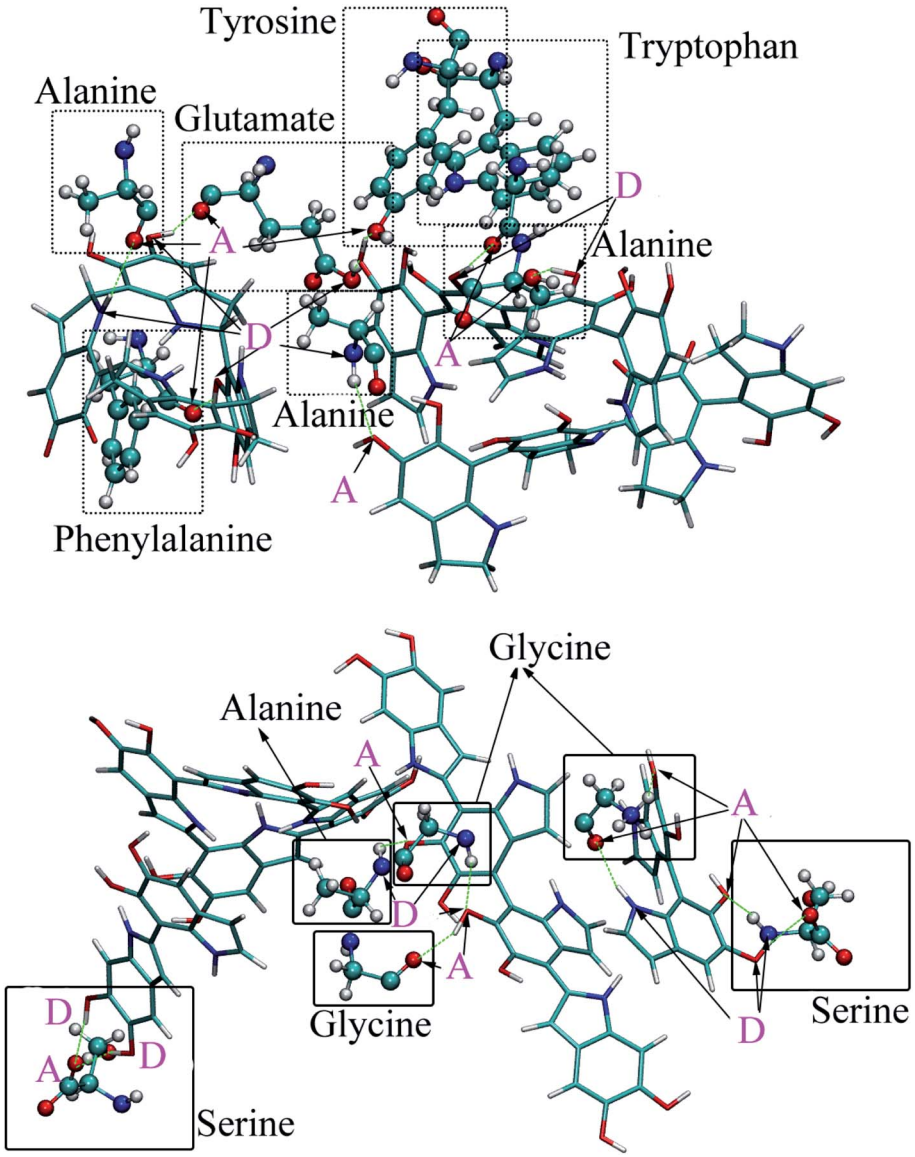

Fig. 5 The detailed information of the hydrogen bonds between dopamine oligomers and silk fibroin (amino acid – ball and stick model; dopamine oligomers – stick model; D: donor; A: acceptor; red – oxygen atom; cyan – carbon atom; blue – nitrogen atom; white – hydrogen atom).

3.2 The binding process of dopamine oligomer with silk fabric surface

3.2.1 Adsorption of dopamine oligomer on the surface of silk fibroin. The final adsorption state of dopamine polymer on silk fibroin surface was shown in Fig. 3. Some dopamine oligomers were adsorbed on silk fibroin surface, and some of them remained in solution. Most of the dopamine oligomers adsorbed on the surface of silk were distributed near the amorphous region (the blue part), which indicated that dopamine oligomers mainly bound to the amorphous region of silk fabric in the process of dyeing modification. The reason for the adsorption of the most oligomers on the amorphous region of the silk fibroin surface was that the crystalline part of the silk fibroin had tighter structures and steric effect for the oligomers.

In order to further understand the adsorption situation of dopamine oligomers to the surface of silk fibroin, the whole silk fibroin, two amorphous regions and one crystalline region were taken as reference molecules, the radial distribution functions (RDF) of dopamine oligomers in different time periods were calculated. For the RDF analysis, the atoms in the amino acid of the crystalline or amorphous regions were the reference parts, and the atoms in the oligomers were the calculating parts. It can be seen from Fig. 4a that the dopamine oligomers gradually approach the silk protein. After 150 ns, the peak value of the RDF no longer increased, but slightly decreased, which indicated that the adsorption had reached dynamic equilibrium. From the comparison of Fig. 4b–d, it can be seen that the dopamine oligomers around the two amorphous regions were relatively closer, and the peak value appeared at about 0.5 nm,

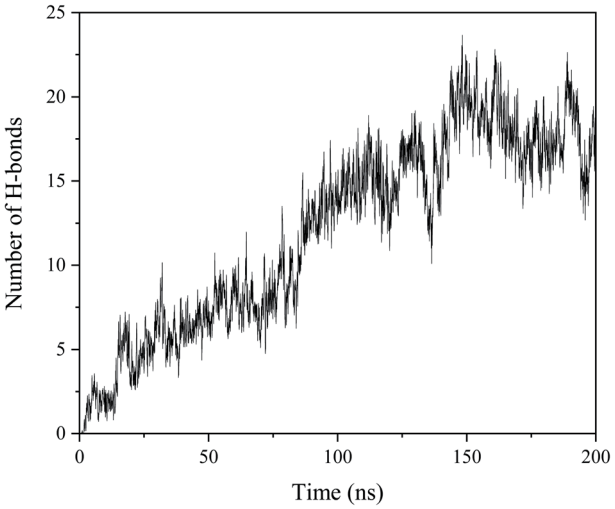

Fig. 6 Changes of the number of hydrogen bonds between dopamine oligomers and silk fibroin over time.

while the peak value of RDF in the crystal region appeared at about 1.0 nm, indicating that the polydopamine molecules were indeed more inclined to adsorb to the amorphous region of silk fibroin.

3.2.2 The interaction between dopamine oligomers and silk protein

(1) Hydrogen bond. The details of the formation of hydrogen bonds in the calculated final state system are shown Fig. 5, and the upper and lower figures respectively represent the binding situation of dopamine oligomers at different positions on the surface of two amorphous regions of silk fibroin. The method to judge the existence of the hydrogen bond was that the donor–acceptor distance should be less than 0.35 nm, and the hydrogen-donor–acceptor angle should be less than 30°. In Fig. 5, the dopamine oligomers could form hydrogen bonds with glycine, alanine, glutamic acid, tyrosine, phenylalanine, tryptophan and serine in silk fibroin. Similar to amino acids, dopamine oligomers contained both amino and hydroxyl groups, so they could be used as both hydrogen bond donor and hydrogen bond acceptor in the process of combination. The calculation results of hydrogen bond formation between dopamine oligomers and silk fibroin are shown in Fig. 6. With the extension of time, dopamine oligomers gradually combined with silk fibroin. After 150 ns, about 20 hydrogen bonds could be formed between dopamine oligomers and silk fibroin, and then they were in a dynamic equilibrium state.

(2) π–π stacking. Since silk fibroin contains amino acids with benzene ring such as tyrosine, phenylalanine and tryptophan, the π–π accumulation between dopamine oligomers and silk fibroin in the final state was calculated, and the calculation results were shown in Fig. 7. It could be seen that the benzene ring of dopamine oligomers could form π–π stacking with the benzene ring of tyrosine and phenylalanine. As shown in Fig. 7a, the angle between the benzene ring planes of the π–π stacking formed by the oligomer and tyrosine was 6.2°, the distance between the center of mass of tyrosine benzene ring and the benzene ring plane of dopamine oligomer was 3.44 Å, and the distance between the center of mass of dopamine oligomer and the benzene ring plane of tyrosine was 3.55 Å, which belonged to the typical π–π stacking. As shown in Fig. 7b, the angle between the benzene ring planes of the π–π stacking formed by the oligomer and phenylalanine was 17.6°. The distance between the centroid of the benzene ring of phenylalanine and the plane of the dopamine oligomer benzene ring was 2.95 Å, and the distance between the centroid of the benzene ring of dopamine oligomers and the plane of the phenylalanine benzene ring was 3.59 Å. Although the angle between the two planes was slightly larger, it was also in line with the range of π–π stacking interaction.

On the whole, two kinds of atoms of the dopamine oligomers could be attached to the amino acids on the silk protein. One was the amino or hydroxyl group which could form hydrogen bonds with the amino acids. The other was the aromatic ring which could form π–π stacking interaction with the amino acids.

3.2.3 The weak interaction between dopamine oligomers.

In order to understand the adsorption form of dopamine oligomers on silk fibroin surface, the aggregation and association of dopamine oligomers in different time were calculated, and the results were shown in Fig. 8a. In this section, the criterion for judging molecular aggregation: when the distance between any atom in a molecule and any atom in another molecule was less than the sum of the van der Waals radius of the two atoms,

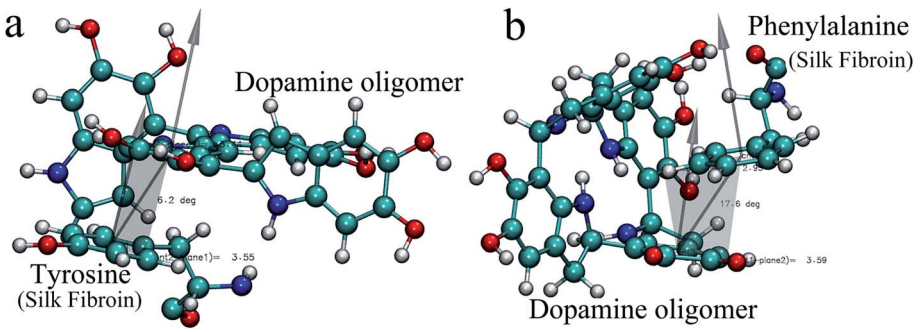

Fig. 7 Detailed information of the π–π stacking interactions between dopamine oligomers and two amino acids of silk fibroin: (a) tyrosine, (b) phenylalanine (red – oxygen atom; cyan – carbon atom; blue – nitrogen atom; white – hydrogen atom).

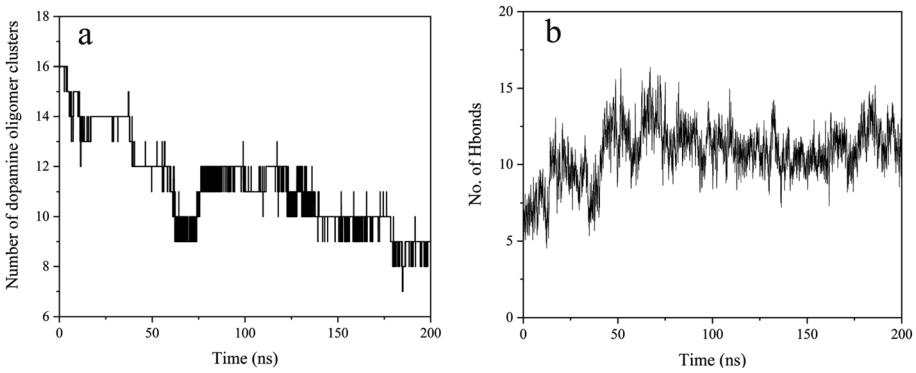

Fig. 8 (a) The aggregation of dopamine oligomers in the adsorption process; (b) changes of the number of hydrogen bonds between dopamine oligomers over time.

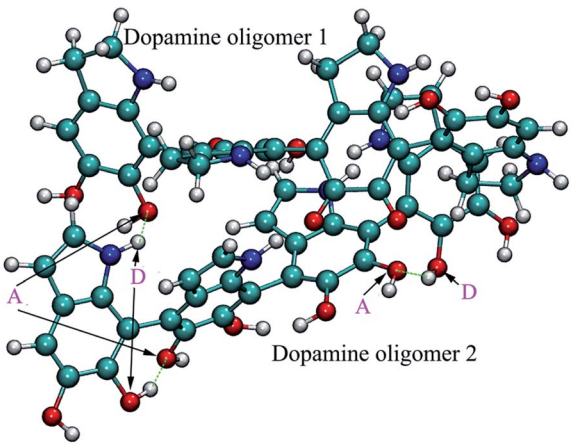

Fig. 9 The detailed information of the hydrogen bonds between dopamine oligomers (D: donor, A: acceptor, red – oxygen atom, cyan – carbon atom, blue – nitrogen atom, white – hydrogen atom).

the two molecules were considered to be a cluster. Since a total of 17 dopamine oligomers were listed (Fig. S1†), it was considered that there were 17 clusters in the initial state, and the number of clusters decreases after the aggregation of dopamine oligomers. It could be seen from the figure that some dopamine oligomers aggregated into aggregates before 50 ns, and then they were in a dynamic equilibrium stage. After 150 ns, the aggregates still existed, and there was a tendency for aggregates to increase. This indicated that during the process of adsorption of dopamine oligomers to the surface of silk fibroin, they may be adsorbed to the surface in the form of aggregates. Similarly, in order to observe the interaction between dopamine oligomers, the calculating results of the number of hydrogen bonds were shown in Fig. 8b. The molecular aggregation reached dynamic equilibrium after 50 ns, and the number of hydrogen bonds (about 12) between dopamine oligomers reached equilibrium. The detailed calculation results of hydrogen bonds formed between dopamine oligomers in the final state were shown in Fig. 9. Hydrogen bonds could be formed between dopamine oligomers through amino and hydroxyl groups, and intramolecular hydrogen bonds could also be formed between adjacent hydroxyl groups of the oligomer itself.

3.2.4 Chemical reaction of dopamine and the oligomers with silk fibroin. Molecules with phenolic structures could react with $-NH_2$ of dopamine by Michael addition, which had been similarly reported in the literature.[33–37] Therefore, the phenol residues of tyrosine in silk fibroin could undergo Michael addition reaction with the $-NH_2$ in dopamine molecules that didn't participate in polymerization in time. At the same time,

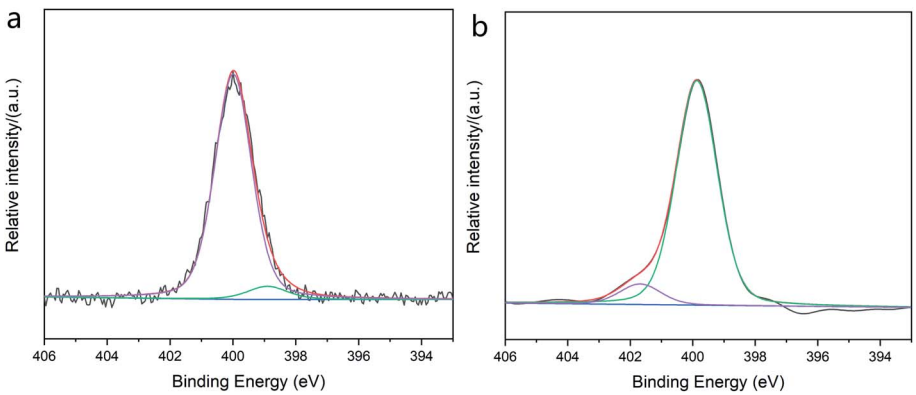

Fig. 10 XPS analysis: high resolution N 1s spectrum of (a) pristine silk fabric and (b) dyed silk fabric (laccase-catalyzed).

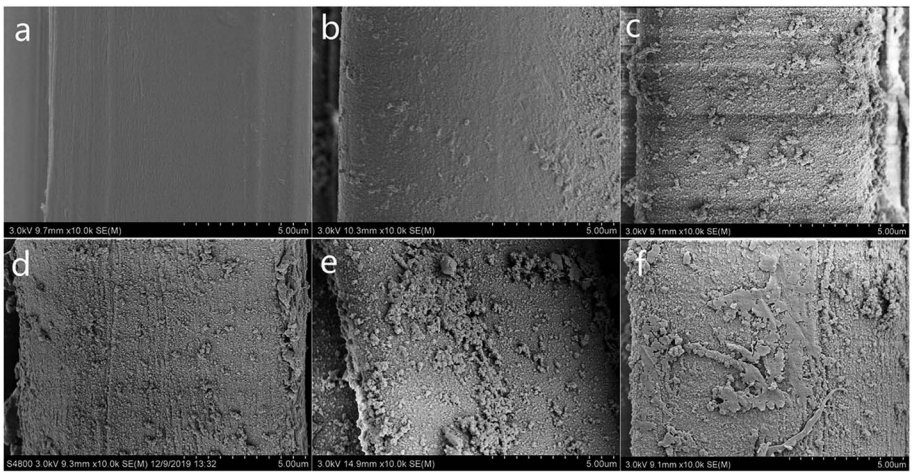

Fig. 11 SEM images of the pristine silk fabric (a), PDA-SF (b) and the surface of the PDA-SF deposited with various metal ions: (c) Ag^{+}, (d) Cu^{2+}, (e) Fe^{3+}, (f) Ni^{2+}.

the $-NH_2$ on the surface of silk fibroin could also undergo Michael addition reaction with polydopamine. Through the analysis of the XPS test (N 1s), as shown in Fig. 10a, there were a large number of –C–NH–C═O (about 95%) and a small amount of $-NH_2$ (about 5%) on the surface of pristine silk fabric, and their peak positions were located at 399.9 eV and 398.9 eV, respectively.[38,39] For the silk fabric after enzymatic dyeing (Fig. 10b), the peak of –C–NH–C– could still be observed on the surface, which came from the amide bond of silk and the imino group in polydopamine. At the same time, $=N^{+}-$ appeared at 401.6 eV, which might be due to the proton transfer of carboxyl group on the silk surface to ═N– in polydopamine molecule.[40,41] However, the peak of $-NH_2$ on the surface of the dyed silk disappeared, and the literature had proved that $-NH_2$ was not detected in the polydopamine catalyzed by laccase,[42] which proved that the $-NH_2$ on the pristine silk surface was completely consumed by Michael addition reaction with polydopamine.

3.3 Deposition of metal ions on enzymatic dopamine modified silk fabric

The silk fabrics (PDA-SF) modified by the above-mentioned enzymatic dopamine polymerization were immersed in the same concentration and different kinds of metal ion solutions (Ag^{+}, Cu^{2+}, Fe^{3+}, Ni^{2+}) for 24 h at room temperature, and the surface morphologies were observed after drying. As shown in Fig. 11a, the surface of the untreated silk fiber was very smooth, without obvious protrusions and foreign objects. After modification by laccase-catalyzed polymerization of dopamine (Fig. 11b), there were a layer of obvious attachments and some convex structures attached to the surface of the silk fiber, but in general, the surface structure was relatively smooth and no special microstructure appeared. However, after the deposition of Ag^{+}, Cu^{2+}, Fe^{3+}, Ni^{2+}, as shown in Fig. 11c–f, the surfaces of the modified silk fibers were covered by a layer of dense granular structure, which greatly increased the surface roughness of the silk fiber. In addition, after the above modification, the surface wettability of silk fabrics also changed to a certain extent. As shown in Table 3, all the PDA-SF modified by metal ion deposition were hydrophobic, and the contact angles were above 130°.

In order to further study the properties of the metal particles deposited on the surface of the PDA-SF fibers, XRD was used to test the crystal structure of the above deposited particles. As shown in Fig. 12a, polydopamine and Ag^{+} formed crystals with good morphology after deposition. The 2θ characteristic peaks at 38.1°, 44.5°, 64.5° and 77.4° were (111), (200), (220) and (311) crystal planes, respectively. This coincided with the crystallization peak of zero-valent nanosilver in the literature,[43–45] indicating that polydopamine had good reducibility, and Ag^{+} could be reduced to a zero-valent state. At the same time, the characteristic peaks at 32.8° and 54.9° also indicated the existence of silver oxide (Ag_2O), which might be the oxide film formed by the oxidation of nano silver surface by oxygen in the air during

Table 3 CA of metal ions deposited on PDA modified silk fabrics (CA/°)

Substrates/ions	SF (°)	PDA-SF (°)	Ag^{+} (°)	Cu^{2+} (°)	Fe^{3+} (°)	Ni^{2+} (°)
CA	0	0	135 ± 2.1	142 ± 2.4	138 ± 2.5	132 ± 1.9
Image of water drop						

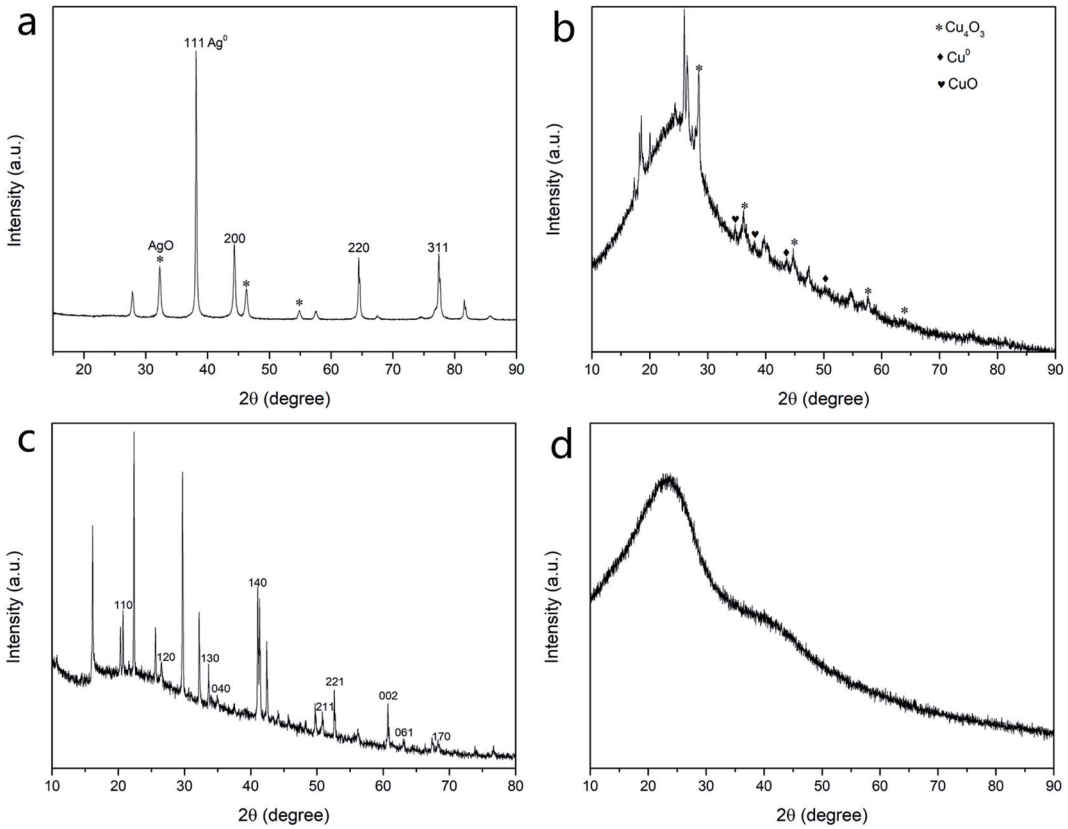

Fig. 12 XRD patterns of particles after 24 hours of enzyme-induced dopamine polymerization combined with various metal ions: (a) Ag^{+}, (b) Cu^{2+}, (c) Fe^{3+}, (d) Ni^{2+}.

preservation.[46,47] The XRD spectrum of the particles formed after the deposition of polydopamine and Cu^{2+} was shown in Fig. 12b, unlike what had been reported in the literature,[48,49] there were no obvious characteristic peaks of zero valent copper appeared. The weak peaks at about 35° and 38° were the characteristic peaks of CuO,[50] and the obvious peaks at about 28.05°, 36°, 44°, 58° and 63.6° could be attributed to the appearance of Cu_4O_3.[51–53] This copper oxide was an uncommon oxide, and it was a metastable oxide, which generally existed together with other copper oxides. Fig. 12c showed the XRD spectrum of particles formed by the deposition of Fe^{3+} and polydopamine, with peaks at 21°, 26.2°, 33.7°, 34.9°, 41.08°, 50.08°, 53°, 61.2°, 63.1° and 68.4° corresponding to (110), (120), (130), (040), (140), (211), (221), (002), (061) and (170) crystal planes of α-FeOOH, respectively.[54,55] This result indicated that the mineralized substance with good crystal structure was formed during the deposition of ferric ion and polydopamine. Fig. 12d showed the XRD spectrum of particles deposited by Ni^{2+} and polydopamine. The wide peak at about 20° to 25° was generated by organic matter.[56] There was no obvious metal crystal in the spectrum, only an inconspicuous peak of the (111) crystal plane (44.5°) of zero-valent Ni appeared.[57] But in general, the composite particles of polydopamine and nickel were mainly amorphous particles.

4. Conclusions

In summary, compared with the traditional polymerization of dopamine under alkaline conditions, the polymerization rate of laccase catalyzed self-polymerization under acidic conditions was greatly increased, and the polymer solution was homogeneous without obvious aggregation. Moreover, the dyeing time of laccase catalyzed dopamine modified silk fabric could be greatly shortened, and the dyeing effect of silk fabric was better and more uniform. The color fastness of the silk fabrics dyed by the two methods was basically the same, but the mechanical properties of the silk fabric after enzymatic dyeing were relatively better maintained. Through molecular dynamics simulation studies, it was found that dopamine polymers were easily combined with the amorphous regions of silk fibroin, and dopamine oligomers and amino acids of silk fibroin could form hydrogen bonds and π–π stacking interactions. Dopamine oligomers would aggregate in the process of adsorption to silk fibroin, and the oligomers might be adsorbed on the surface of silk fibroin in the form of aggregates. In addition, dopamine oligomers could form intermolecular and intramolecular hydrogen bonds through amino groups and hydroxyl groups. Meanwhile, $-NH_2$ on the surface of silk fibroin would also be consumed due to the Michael addition reaction with dopamine and its oligomers. After polydopamine dyed silk fabrics were reacted with Ag^{+}, Cu^{2+}, Fe^{3+}, and Ni^{2+}, the silk fabrics had good

hydrophobicity, which was attributed to the rough structure of hybrid particles with different crystal structures formed by polydopamine and metal ions on the silk fiber surfaces.

Author contributions

Qingqing Zhou: methodology, data curation, writing – original draft, project administration. Wen Wu: investigation, data curation. Tieling Xing: validation, writing – review & editing.

Conflicts of interest

There are no conflicts of interest to declare.

Acknowledgements

This work was supported by the Open Project Program of Key Laboratory of Yarn Materials Forming and Composite Processing Technology of Zhejiang Province (No. 002CD1902-12-3-048) and Public Welfare Research Project of Jiaxing City (No. 2019AD32011).

Notes and references

1 B. Yan, Q. Zhou, X. Zhu, J. Guo, M. S. Mia, X. Yan, G. Chen and T. Xing, *Appl. Surf. Sci.*, 2019, **483**, 929–939.
2 F. Bernsmann, V. Ball, F. Addiego, A. Ponche, M. Michel, J. J. d. A. Gracio, V. Toniazzo and D. Ruch, *Langmuir*, 2011, **27**, 2819–2825.
3 Q. Wei, F. Zhang, J. Li, B. Li and C. Zhao, *Polym. Chem.*, 2010, **1**, 1430–1433.
4 C. Zhang, Y. Ou, W.-X. Lei, L.-S. Wan, J. Ji and Z.-K. Xu, *Angew. Chem., Int. Ed.*, 2016, **55**, 3054–3057.
5 Y. Zhou, J. Zhang, R.-C. Tang and J. Zhang, *Ind. Crops Prod.*, 2015, **64**, 224–232.
6 Y. Zhou and R.-C. Tang, *Dyes Pigm.*, 2016, **134**, 203–211.
7 F. Wu, L. Su, P. Yu and L. Mao, *J. Am. Chem. Soc.*, 2017, **139**, 1565–1574.
8 H. Huang, L. Lei, J. Bai, L. Zhang, D. Song, J. Zhao, J. Li and Y. Li, *Chin. J. Chem. Eng.*, 2021, **29**, 167–175.
9 D. Singh and N. Gupta, *Biologia*, 2020, **75**, 1183–1193.
10 R. Pulicharla, R. K. Das, S. Kaur Brar, P. Drogui and R. Y. Surampalli, *Chem. Eng. J.*, 2018, **347**, 828–835.
11 A. N. Kagalkar, R. V. Khandare and S. P. Govindwar, *RSC Adv.*, 2015, **5**, 80505–80517.
12 M. Yuan, Q. Wang, J. Shen, E. Smith, R. Bai and X. Fan, *Text. Res. J.*, 2018, **88**, 1834–1846.
13 N. A. Ibrahim, B. M. Eid, M. S. Abdel Aziz, S. M. Hamdy and S. E. Abd Allah, *Cellulose*, 2018, **25**, 6207–6220.
14 Y. Nong, Z. Zhou, J. Yuan, P. Wang, Y. Yu, Q. Wang and X. Fan, *Fibers Polym.*, 2020, **21**, 1927–1937.
15 T. Zhang, R. Bai, Q. Wang, X. Fan, P. Wang, J. Yuan and Y. Yu, *Color. Technol.*, 2017, **133**, 65–72.
16 K. Rafińska, P. Pomastowski, J. Rudnicka, A. Krakowska, A. Maruśka, M. Narkute and B. Buszewski, *Food Chem.*, 2019, **289**, 16–25.
17 V. V. Milevskaya, S. Prasad and Z. A. Temerdashev, *Microchem. J.*, 2019, **145**, 1036–1049.
18 O. Sytar, I. Hemmerich, M. Zivcak, C. Rauh and M. Brestic, *Saudi J. Biol. Sci.*, 2018, **25**, 631–641.
19 C. Araya-Cloutier, J.-P. Vincken, R. van Ederen, H. M. W. den Besten and H. Gruppen, *Food Chem.*, 2018, **240**, 147–155.
20 F. C. Biluca, J. S. de Gois, M. Schulz, F. Braghini, L. V. Gonzaga, H. F. Maltez, E. Rodrigues, L. Vitali, G. A. Micke, D. L. G. Borges, A. C. O. Costa and R. Fett, *J. Food Compos. Anal.*, 2017, **63**, 89–97.
21 S. Huang, Y. Zhang, J. Shi and W. Huang, *ACS Sustainable Chem. Eng.*, 2016, **4**, 676–681.
22 Q. Zhou, W. Wu, S. Zhou, T. Xing, G. Sun and G. Chen, *Chem. Eng. J.*, 2020, **382**, 122988.
23 X. Yu, Q.-Z. Zhong, H.-C. Yang, L.-S. Wan and Z.-K. Xu, *J. Phys. Chem. C*, 2015, **119**, 3667–3673.
24 D. Chai, Z. Xie, Y. Wang, L. Liu and Y.-J. Yum, *ACS Appl. Mater. Interfaces*, 2014, **6**, 17974–17984.
25 Y. Cheng, L.-D. Koh, D. Li, B. Ji, Y. Zhang, J. Yeo, G. Guan, M.-Y. Han and Y.-W. Zhang, *ACS Appl. Mater. Interfaces*, 2015, **7**, 21787–21796.
26 K. Lindorff-Larsen, S. Piana, K. Palmo, P. Maragakis, J. L. Klepeis, R. O. Dror and D. E. Shaw, *Proteins: Struct., Funct., Bioinf.*, 2010, **78**, 1950–1958.
27 J. Wang, R. M. Wolf, J. W. Caldwell, P. A. Kollman and D. A. Case, *J. Comput. Chem.*, 2004, **25**, 1157–1174.
28 J. Wang, W. Wang, P. A. Kollman and D. A. Case, *J. Am. Chem. Soc.*, 2001, **222**, U403.
29 C. I. Bayly, P. Cieplak, W. Cornell and P. A. Kollman, *J. Phys. Chem.*, 1993, **97**, 10269–10280.
30 A. K. Chew and R. C. Van Lehn, *Front. Chem.*, 2019, **7**, 439.
31 Z. Ahmad, M. S. Naeem, A. Jabbar, *et al.*, *Fibers Tech. Text.*, 2020, 201–220.
32 X. Xueliang, *Handb. Fibrous Mater.*, 2020, 37–74.
33 H. Abe and H. Yabu, *Langmuir*, 2021, **37**, 6201–6207.
34 H. Pang, S. Zhao, L. Mo, Z. Wang, W. Zhang, A. Huang, S. Zhang and J. Li, *J. Appl. Polym. Sci.*, 2020, **137**, 48785.
35 H. Liu, M. Yuan, J. Sonamuthu, S. Yan, W. Huang, Y. Cai and J. Yao, *New J. Chem.*, 2020, **44**, 884–891.
36 S. Chen, S. Liu, L. Zhang, Q. Han, H. Liu, J. Shen, G. Li, L. Zhang and Y. Yang, *Chem. Eng. J.*, 2020, **399**, 125795.
37 H. Pang, S. Zhao, T. Qin, S. Zhang and J. Li, *Polymers*, 2019, **11**, 1536.
38 J. S. Stevens, A. C. de Luca, M. Pelendritis, G. Terenghi, S. Downes and S. L. M. Schroeder, *Surf. Interface Anal.*, 2013, **45**, 1238–1246.
39 P. Amornsudthiwat, R. Mongkolnavin, S. Kanokpanont, J. Panpranot, C. S. Wong and S. Damrongsakkul, *Colloids Surf., B*, 2013, **111**, 579–586.
40 J. S. Stevens, S. J. Byard and S. L. M. Schroeder, *J. Pharm. Sci.*, 2010, **99**, 4453–4457.
41 Y. Liu, K. Ai and L. Lu, *Chem. Rev.*, 2014, **114**, 5057–5115.
42 F. Li, Y. Yu, Q. Wang, J. Yuan, P. Wang and X. Fan, *Enzyme Microb. Technol.*, 2018, **119**, 58–64.
43 A. C. Patel, S. Li, C. Wang, W. Zhang and Y. Wei, *Chem. Mater.*, 2007, **19**, 1231–1238.

44 C. Liu, C. Cao, X. Luo and S. Luo, *J. Hazard. Mater.*, 2015, **285**, 319–324.
45 Y. Chen, G. Zhu, M. Hojamberdiev, J. Gao, R. Zhu, C. Wang, X. Wei and P. Liu, *J. Hazard. Mater.*, 2018, **344**, 42–54.
46 D. Vidyasagar, S. G. Ghugal, A. Kulkarni, P. Mishra, A. G. Shende, Jagannath, S. S. Umare and R. Sasikala, *Appl. Catal., B*, 2018, **221**, 339–348.
47 W. Shen, P. Li, H. Feng, Y. Ge, Z. Liu and L. Feng, *Mater. Sci. Eng., C*, 2017, **75**, 610–619.
48 J. Yang, H. Xu, L. Zhang, Y. Zhong, X. Sui and Z. Mao, *Surf. Coat. Technol.*, 2017, **309**, 149–154.
49 X. Liu, A. Wang, L. Li, T. Zhang, C.-Y. Mou and J.-F. Lee, *J. Catal.*, 2011, **278**, 288–296.
50 W. Chen, Z. Fan and Z. Lai, *J. Mater. Chem. A*, 2013, **1**, 13862–13868.
51 F. Li, Q. Chang, N. Li, C. Xue, H. Liu, J. Yang, S. Hu and H. Wang, *Chem. Eng. J.*, 2020, **394**, 125045.
52 M. S. Abdel-wahab and A. H. Hammad, *Mater. Today Commun.*, 2021, **28**, 102605.
53 L. Zhao, H. Chen, Y. Wang, H. Che, P. Gunawan, Z. Zhong, H. Li and F. Su, *Chem. Mater.*, 2012, **24**, 1136–1142.
54 B. Wang, H. Wu, L. Yu, R. Xu, T.-T. Lim and X. W. Lou, *Adv. Mater.*, 2012, **24**, 1111–1116.
55 B. Tang, G. Wang, L. Zhuo, J. Ge and L. Cui, *Inorg. Chem.*, 2006, **45**, 5196–5200.
56 Z. Wang, C. Fang and M. Megharaj, *ACS Sustainable Chem. Eng.*, 2014, **2**, 1022–1025.
57 M. Jia, C. Choi, T.-S. Wu, C. Ma, P. Kang, H. Tao, Q. Fan, S. Hong, S. Liu, Y.-L. Soo, Y. Jung, J. Qiu and Z. Sun, *Chem. Sci.*, 2018, **9**, 8775–8780.